Electrical Power and Energy Systems 162 (2024) 110295

Contents lists available at ScienceDirect

International Journal of Electrical Power and Energy Systems

journal homepage: www.elsevier.com/locate/ijepes

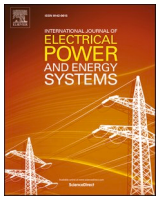

Development of coordinated control method based on Graph search method between EV and DG for voltage regulation

Jisoo Kim *, Jean Mahseredjian

Polytechnique Montreal, Montreal QC H3T 1J4, Canada

ARTICLE INFO

Keywords:
Coordinated Control
Graph Search Method
Distributed Generation
Distribution System
Electric Vehicle

ABSTRACT

In this paper, a study is conducted to solve voltage problems that may occur, when large-scale Distributed Generations (DGs) and Electric Vehicles (EVs) are connected to the distribution system, through coordinated control between DGs and EVs. Using the Graph Search Method (GSM), the voltage problem was solved through the reactive power control of EVs and DGs in the near area where the voltage problem occurred. As a result, it was possible to obtain a result with high robustness against the change of the topology and reduction of the total loss of distribution system. In addition, when the voltage problem cannot be solved by only reactive power control, the active power control was performed for EVs and DGs included in a specific divided system of the conventional distribution system using the GSM to maintain the voltage within the normal range. Finally, to verify the performance of the proposed method, the whole algorithm was implemented by linking the Open Source Distribution System Simulator (OpenDSS), and the MATLAB.

1. Introduction

To overcome environmental problems worldwide, the penetration of Distributed Generations (DGs) using Renewable Energy Sources(RESs) in the distributions system is increasing. Similarly, in the transportation sector, the shift from conventional internal combustion vehicles to Electric Vehicles (EVs) is accelerating to support decarbonization [1]. However, the connection of large-scale DGs and EVs to the distribution system has very high variability of output and load compared to existing power sources and loads, which can cause overvoltage or undervoltage situations [2,3]. As the penetration rate of Distributed Generations (DGs) and Electric Vehicles (EVs) increases, the excess generation exceeding demand will flow into the power system, resulting in reverse power flow. This phenomenon leads to overvoltage conditions within the power system. In a typical radial system, voltage tends to decrease with increasing distance from the main power source due to impedance. Consequently, power system operators can easily manage the voltage within the prescribed upper and lower limits of the voltage standard. However, the integration of DGs and EVs can lead to scenarios where the generation and load levels exceed expectations, potentially causing overvoltage and undervoltage conditions that surpass the established standards for the power system. This issue must be addressed as it negatively impacts the quality of power supplied to the load and compromises the stability of the entire power system.

In order to solve these voltage problems, there are research on the improvement of various algorithms of conventional voltage regulators such as On Load Tap Changer (OLTC) [4–7]. However, since OLTC has a centralized control tendency and it operates based on unidirectional power flow, reverse power flow which may occur due to high penetration of DGs may cause malfunction of conventional voltage regulator. As a result, it may adversely affect consumers and electrical devices in the whole distribution system [4]. Especially, as the distribution system evolves with the integration of distributed power sources and electric vehicles, its complexity grows, making centralized voltage management through OLTC connections to the main power source increasingly challenging. Consequently, there arises a demand for decentralized solutions where distributed power sources or electric vehicles autonomously control reactive power, thereby facilitating local voltage regulation. So, the IEEE 1547, which is international standard, was revised in 2018 so that DGs, which were initially prohibited from supporting reactive power, can support reactive power to solve the voltage problem [8]. Research related to reactive power control of DGs is generally conducted so that DGs can control reactive power corresponding to the voltage measured at the Point of Common Coupling (PCC) by using the volt/VAR characteristic curve through optimization process [9–13]. This approach optimizes the volt/VAR characteristic

* Corresponding author.
E-mail address: kjs7107@naver.com (J. Kim).

https://doi.org/10.1016/j.ijepes.2024.110295
Received 1 March 2024; Received in revised form 5 July 2024; Accepted 6 October 2024
Available online 19 October 2024

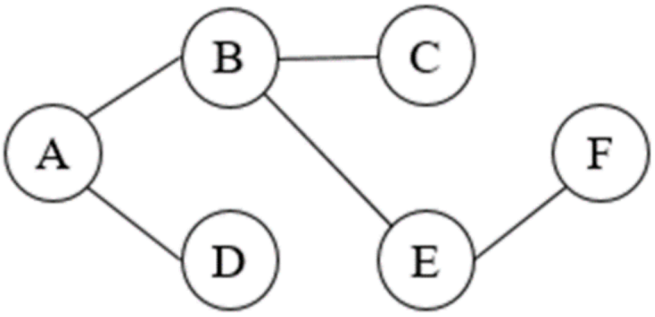

Fig. 1. Example of graph search method.

curve of smart inverters by employing various objective functions, such as minimizing voltage fluctuations, power losses, or economic costs. However, these optimizations are typically computed based on daily or yearly averages, which may not promptly adapt to fluctuations in the output of DGs, EVs or address immediate power system contingencies. Furthermore, due to the increasing complexity of distribution systems, optimization algorithms often require extensive time to yield results. This delay results in a misalignment with the real-time operational demands of the globally expanding distribution automation systems. Especially, this research direction has a disadvantage in that it is difficult to solve the voltage problem when overvoltage continues to occur due to an increase in the capacity of the DGs only with the limited reactive power that can be maximally output from the DGs themselves. In addition, the results of optimization don't reflect the real-time situation and don't respond to changes in system topology. As a result, other electrical devices that can regulate the voltage, not just DGs, should control the voltage together with the DGs for real-time. However, conventional voltage regulators are very difficult to solve for all the distributed overvoltage areas that DGs can cause.

In this paper, voltage regulating method using EVs was performed to solve these problems, and the EVs can output or absorb the reactive power and active power when connected to a smart charging station [14]. The conventional research of regulating the voltage in the distribution line using the EVs is largely divided into two. The first is a method in which the Optimal Power Flow(OPF) problem of the distribution system is calculated. The optimal absorbing or injecting active and reactive power is calculated at each EV's aggregator, and the EVs output the corresponding reference [14–16]. However, this method of solving OPF is difficult to apply in real time due to calculation time, so it is suitable for scheduling the EV charging and discharging for the next day, as used in the literature. Serious fluctuations, in generation of DGs and load of EVs, reduced the reliability of such algorithms, and even if the algorithm used, an auxiliary algorithm that controls the voltage in real time is required. The second method is to apply the optimized volt/VAR characteristic curve used in the smart inverter to smart charging station in the same way [17–19]. However, the methodology employing optimization algorithms involves pre-selecting an optimized volt/VAR characteristic curve prior to system operation, thereby posing challenges in responding in real-time to future distribution systems characterized by high penetration of DGs and EVs with volatile outputs. This difficulty arises from the slow calculation speed of optimization algorithms and the need to additionally consider constraints for dynamic system changes. Like this, the method using the optimized volt/VAR characteristic curve is also difficult to respond to rapidly changing system situation, and it is difficult to respond to changes in system topology. In addition, in most conventional literature which uses EVs to regulate voltage, all EVs participate in reactive power control. This research increases the reactive power through the distribution line, resulting in reduced transmission capacity. Also, it may interfere with the smooth power flow and cause additional heat and transmission loss [20].

Therefore, the proposed algorithm in this paper has solved such a problem, and the contribution of this paper is as follows.

1) For real-time, a coordinated volt/VAR and volt/watt control method between EVs and DGs for voltage regulation was presented, and when the voltage problem was not solved with reactive power alone, the voltage problem was solved by controlling the additional active power.
2) Voltage regulating was performed using only near EVs and DGs to the area where the voltage problem occurred. As a result, proposed method was able to reduce system loss compared to all EVs operating.

Even if the system topology changes, it is possible to re-find the EVs and DGs adjacent to the area where the voltage problem occurred by using Graph Search Method(GSM) without an additional algorithm.

2. Graph search method

The graph search method is mainly applied to data structures, which are used for efficiently managing and structuring data to be processed by a computer. There are two types of search methods to find a route from a starting node to target node: Depth-First Search (DFS) and Breadth-First Search (BFS) [21]. To perform the GSM, the connection information between each element should be configured in matrix. For example, when a structure like Fig. 1 exists, Fig. 1 can also be expressed as Matrix (1). If each pair of nodes is connected, the corresponding matrix entry is not 0; otherwise, it is 0. The completed matrix is symmetric [21].

$$\begin{array}{c|cccccc} & A & B & C & D & E & F \\ A & 0 & 1 & 0 & 1 & 0 & 0 \\ B & 1 & 0 & 1 & 0 & 1 & 0 \\ C & 0 & 1 & 0 & 0 & 0 & 0 \\ D & 1 & 0 & 0 & 0 & 0 & 0 \\ E & 0 & 1 & 0 & 0 & 0 & 1 \\ F & 0 & 0 & 0 & 0 & 1 & 0 \end{array} \quad (1)$$

2.1. Breadth first search

In this paper, BFS, using Matrix (1) with distance information, is used to solve the voltage problem with specific EVs and DGs. BFS is a method that begins by sequentially searching all nodes adjacent to the start node; if the information isn't found, searching continues from the adjacent nodes sequentially [21]. If BFS is applied to Fig. 1, the search proceeds in the order of A-B-D-C-E-F.

2.2. Depth first search

DFS is a method of searching deeply by selecting one edge from each node. If it is impossible to go any further, the search returns to the last branch found during the search and starts the search along another edge. If DFS is applied to Fig. 1, the search proceeds in the order of A-B-C-E-F-D.

3. Proposed coordinated control between EVs and DGs using reactive power

3.1. Selecting the operation sequence of EVs and DGs

When an overvoltage or undervoltage occurs according to (2), utility will receive this information on which bus the problem occurred.

$$0.95p.u < V < 1.05p.u \quad (2)$$

The point where the largest overvoltage occurs will be the PCC of DG and where the smallest undervoltage occurs will be the one point of the line. Therefore, if there is a DG connected to the bus corresponding to the overvoltage, the DG location becomes the starting point of the BFS.

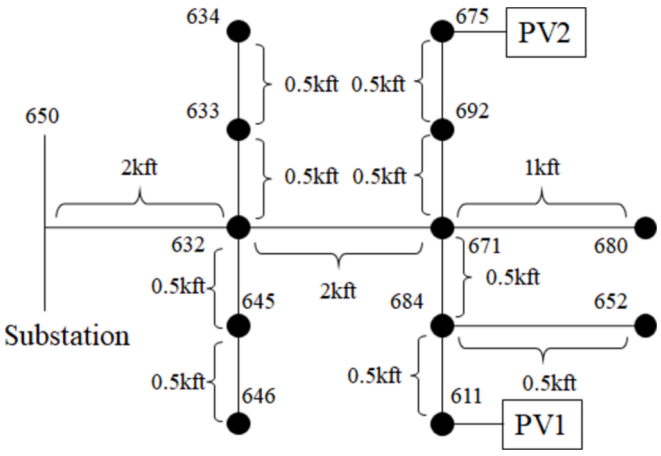

Fig. 2. IEEE 13 bus test system with Photovoltaics(PV).

Table 1
Operation sequence of reactive power.

Order	1	2	3	4	5
Unit	PV2	#675 bus	#692 bus	#671 bus	#684 bus
Order	6	7	8	9	10
Unit	#680	#611 bus	#652 bus	PV1	#632 bus
Order	11	12	13	14	15
Unit	#633	#645 bus	#634 bus	#646 bus	#650 bus

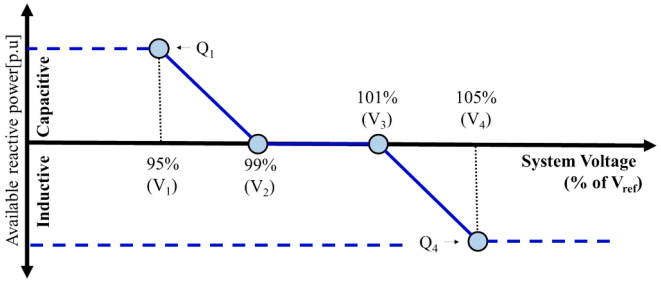

Fig. 3. Volt/VAR curve for active priority mode.

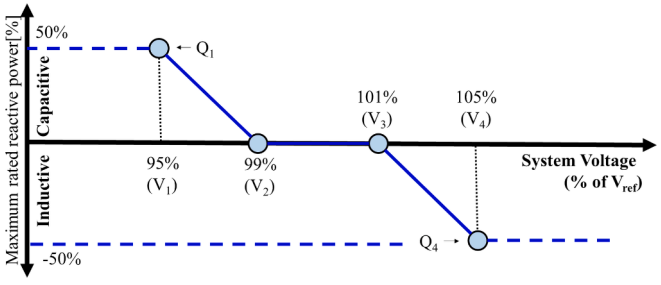

Fig. 4. Volt/VAR curve for reactive priority mode.

On the contrary, the bus with the lowest undervoltage is the starting point of BFS for each subdivision determined in Section 4. At this time, the search is based on BFS, but the algorithm is implemented so that the searching order can be updated according to the accumulated distance from the starting point. These processes can be easily seen in Fig. 2.

If it is assumed that overvoltage has occurred on bus #675, the starting point of the BFS is PV2. Therefore, BFS searches PV2 – #675bus – #692bus – #671bus in order according to the system connection information. At this time, in the case of searching from #671bus, three search paths(#632, #680, #684 bus) exist. When there are multiple paths for the search, the search proceeds in the order of the closest distance to search for the nearest EV and DGs. As a result, BFS performs searches in the order of #684, #680, and #632bus. After that, when searching for #684bus, the accumulated distance from PV2 to #652 and #611bus is shorter than the accumulated distance from PV2 to #632bus, so #611 and #652bus has priority over the #632bus. To perform this process, it is necessary to add up the lengths of the paths in the search process. Finally, the priority for reactive power control of each bus starting from PV2 where the overvoltage occurred is as follows. The reason for the search according to the distance is that the voltage deviation increases as the distribution line gets longer, so when the control target is far away from the problem area, more reactive power, and losses from the line increase.

3.2. *Proposed Volt/VAR control of EVs and DGs*

When the voltage problem occurs in distribution system, the operation sequence is determined based on Table 1, and volt/VAR operations of EVs and DGs are sequentially performed. To elucidate the Volt/VAR function of a smart inverter, it is essential to comprehend the operational principles of reactive power priority mode and active power priority mode. The maximum reactive power supported by the smart inverter's Volt/VAR function is defined by the EPRI as follows:

1) Reactive power priority mode

In this mode, the maximum reactive power supported by the smart inverter corresponds to its maximum rated reactive power. If the total apparent power exceeds the inverter's capacity due to the required reactive power, the inverter prioritizes reactive power output at the expense of active power.

2) Active power priority mode

Here, the maximum reactive power is also the maximum rated reactive power that the inverter can output. However, the maximum reactive power is achievable only when the active power is zero. As the output of active power increases, the amount of reactive power that can be output correspondingly decreases.

When the voltage problem is solved during sequential control, only specific EVs and DGs can participate for the control. At this time, the volt/VAR control operates in the active power priority mode to minimize the curtailment amount of the active power as much as possible. Therefore, in the volt/VAR characteristic curve as shown in Fig. 3, it can be seen that y-axis is the amount of available reactive power. In addition, since this paper isn't a paper to optimize the volt/VAR characteristic curve, the following volt/VAR curve, which is generally used, is used [19].

If the active power priority mode is performed and the voltage is not maintained within the normal range even though all DGs and EVs have performed reactive power control, then, according to Table 1, the reactive power priority mode is sequentially performed to perform reactive power control. At this time, volt/VAR control is performed according to Fig. 4, and since it is reactive power priority mode, the y-axis is the maximum rated reactive power.

4. Proposed coordinated control between EVs and DGs using active power

When DGs and EVs are connected to the distribution system on a large scale, the general reason for the voltage problem is that there is a large amount of generation of DGs or a load of EVs. Therefore, if the voltage problem cannot be solved even by using reactive power control, the generation should be curtailed, or the load should be cut off. As a result, in this section, curtailment of DGs using active power and cut-off method EV are proposed. Since this method is controlled after

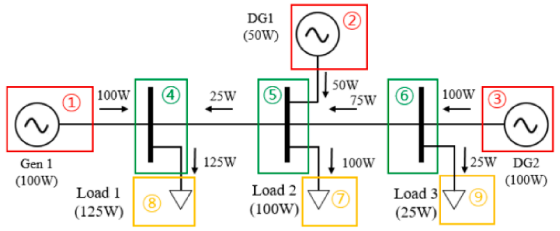

(a) Calculating power flow

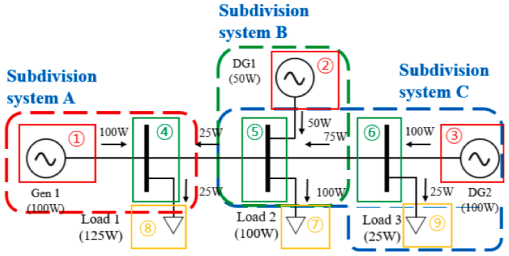

(b) Performing DFS from generator to common bus

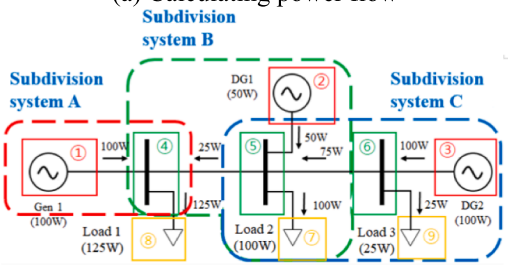

(c) Determining the subdivision group for the next element to #5 common bus

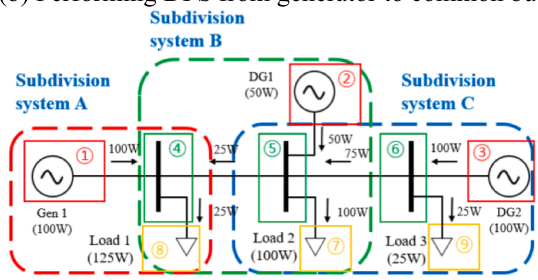

(d) Determining the subdivision group for the next element to #4 common bus

Fig. 5. Example of distribution system division process.

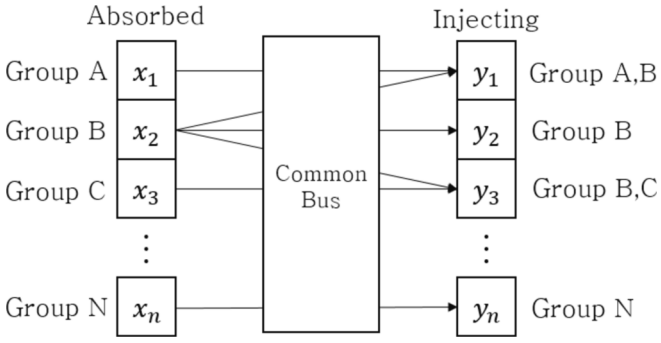

Fig. 6. Matching between absorbed and injecting power in the common bus.

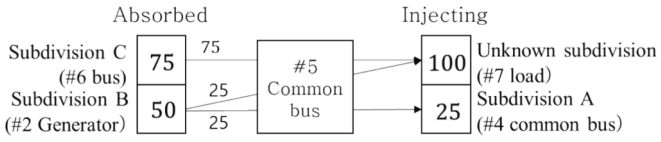

Fig. 7. Matching between absorbed and injecting power in the #5 common bus.

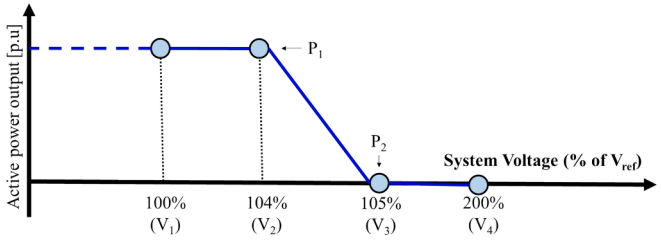

Fig. 8. Volt/Watt curve for DGs to solve overvoltage.

performing reactive power control, it is necessary to shorten the time for real-time control. For this purpose, a strategy for subdividing the distribution system is proposed and control units included in the same

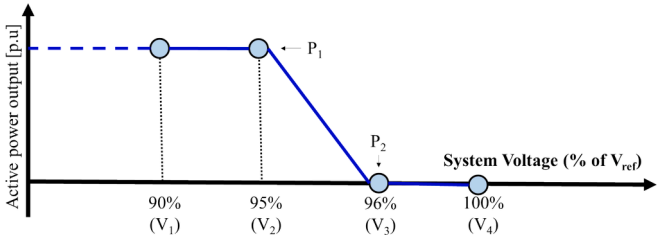

Fig. 9. Volt/Watt curve for EVs to solve undervoltage.

subdividing system can control active power together. In addition, it is possible to distribute the control burden for the active power of the individual DG and EV units through this method.

4.1. Division of distribution systems

The proposed method is a method of dividing each area in which the supply–demand balance is maintained. Currently, various power companies can monitor the real-time power metrics for each busbar within their distribution systems using supervisory control and data acquisition systems, such as Supervisory Control and Data Acquisition (SCADA). At this point, each power company's central management system can utilize the acquired data to construct the following matrix. In order to use this method information on power flow should be put in the connection information between each element in Matrix (1) as shown in Matrix (3). At this time, the direction of absorbing and injecting power should be determined by including the sign. The distribution system is divided if the search is carried out in the direction of power flow starting from each DG until the search is no longer possible.

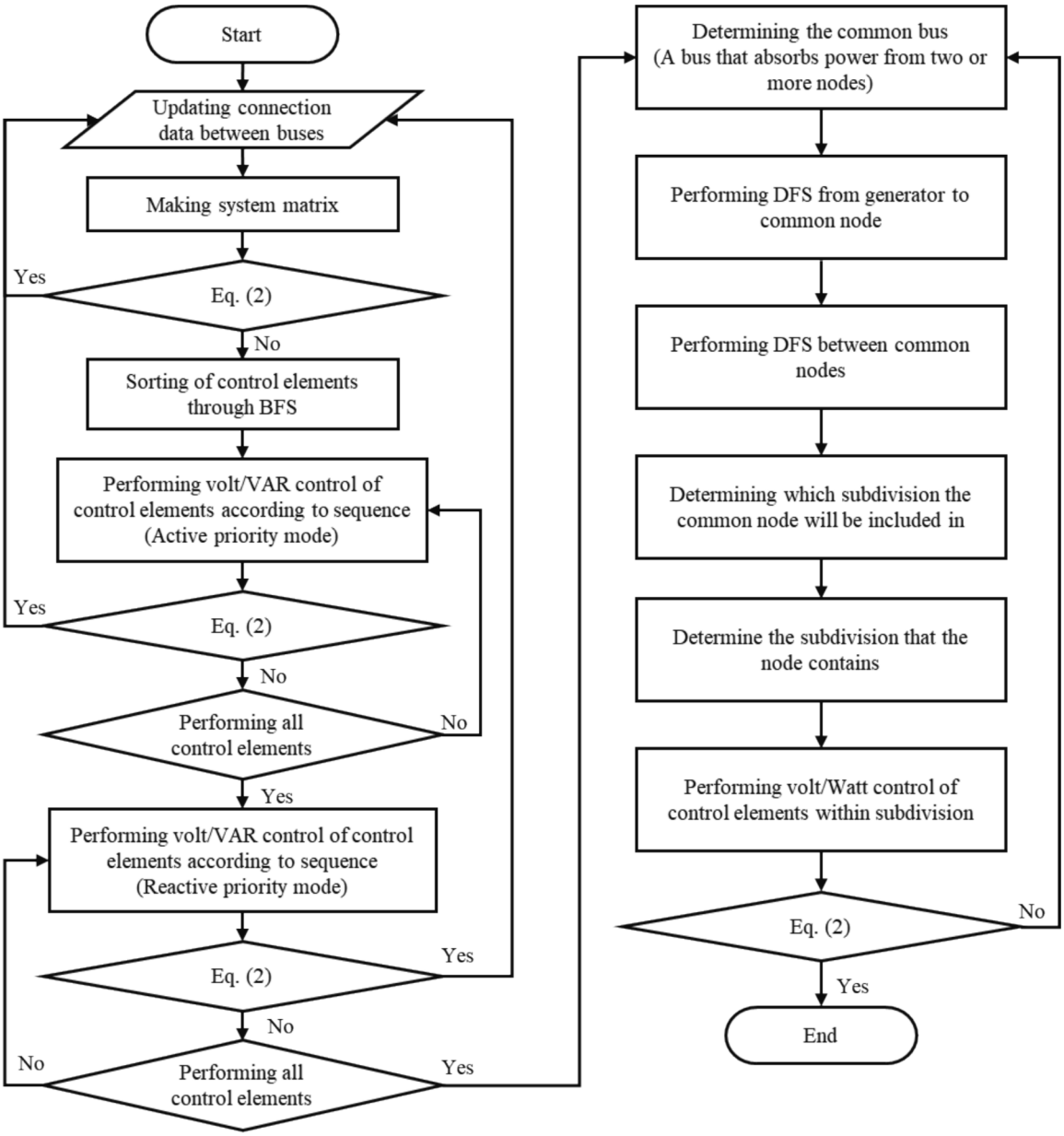

Fig. 10. Overall flowchart proposed in this paper.

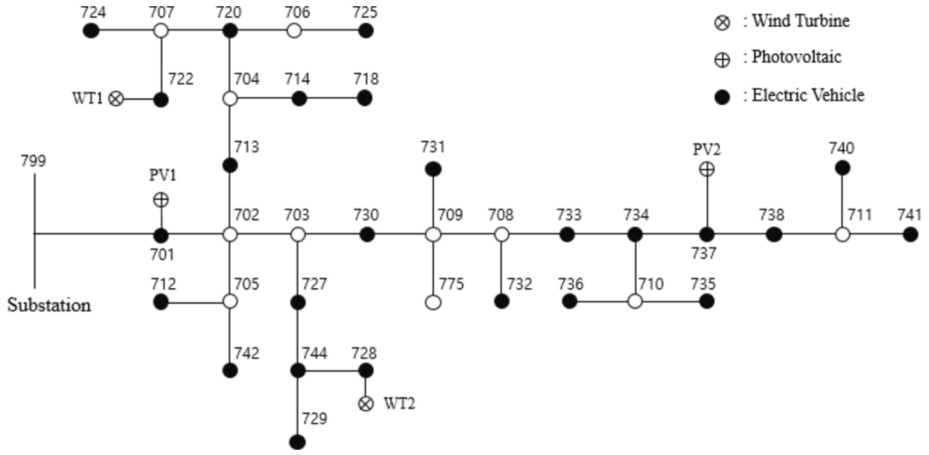

Fig. 11. Simulated IEEE 37 bus test system.

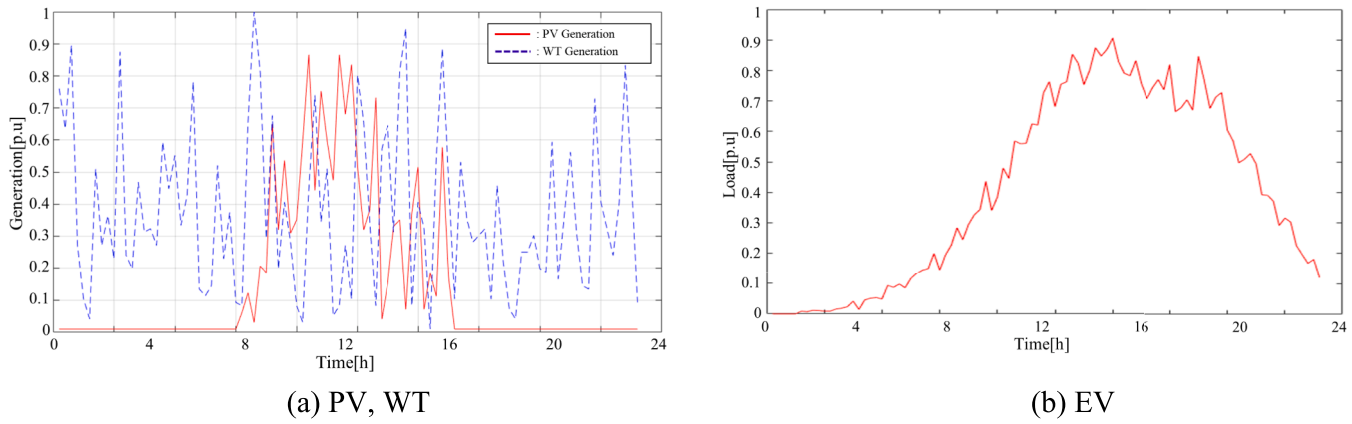

(a) PV, WT (b) EV

Fig. 12. PV, WT and EV daily profile.

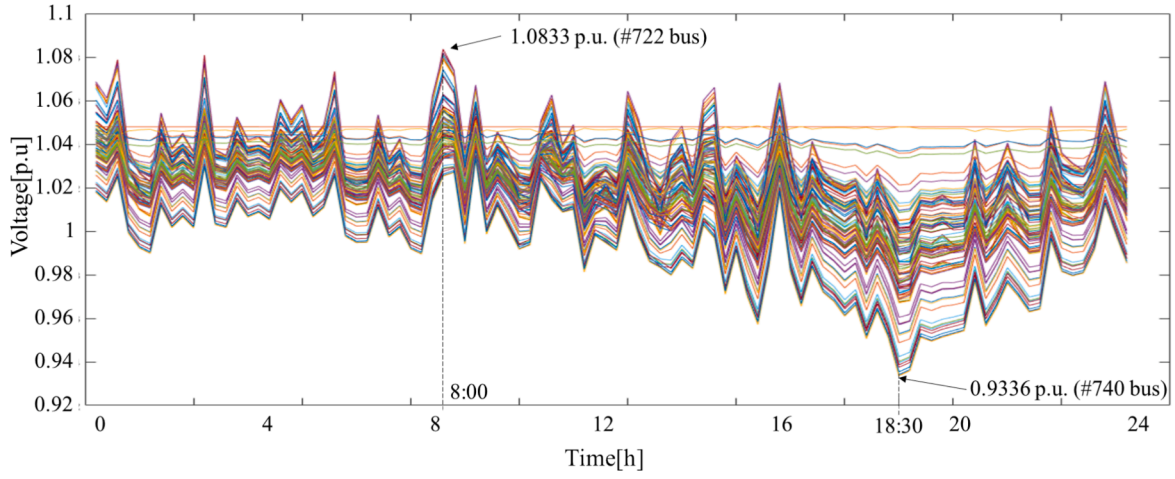

Fig. 13. Voltage profile before applying proposed method.

Table 2
Bus searching results from WT1.

Order	1	2	3	4	5	6	7	8
No.	WT1	#722 bus	#724 bus	#720 bus	#714 bus	#725 bus	#713 bus	#718 bus
Order	9	10	11	12	13	14	15	16
No.	#712 bus	#742 bus	PV1	#701 bus	#727 bus	#744 bus	#730 bus	WT2
Order	17	18	19	20	21	22	23	24
No.	#728 bus	#729 bus	#731 bus	#732 bus	#733 bus	#734 bus	#737 bus	PV2
Order	25	26	27	28	29			
No.	#735 bus	#738 bus	#740 bus	#736 bus	#741 bus			

$$\begin{array}{c|ccccccccc} & 1 & 2 & 3 & 4 & 5 & 6 & 7 & 8 & 9 \\ 1 & 0 & 0 & 0 & 100 & 0 & 0 & 0 & 0 & 0 \\ 2 & 0 & 0 & 0 & 0 & 50 & 0 & 0 & 0 & 0 \\ 3 & 0 & 0 & 0 & 0 & 0 & 100 & 0 & 0 & 0 \\ 4 & -100 & 0 & 0 & 0 & -25 & 0 & 0 & 125 & 0 \\ 5 & 0 & -50 & 0 & 25 & 0 & -75 & 100 & 0 & 0 \\ 6 & 0 & 0 & -100 & 0 & 75 & 0 & 0 & 25 & 0 \\ 7 & 0 & 0 & 0 & 0 & -100 & 0 & 0 & 0 & 0 \\ 8 & 0 & 0 & 0 & -100 & 0 & 0 & 0 & 0 & 0 \\ 9 & 0 & 0 & 0 & 0 & 0 & -25 & 0 & 0 & 0 \end{array} \quad (3)$$

The procedure for this process is explained in Fig. 5 as follows. Each number of elements is arbitrarily for convenience of description.

1) Perform power flow analysis on the distribution system. If there are two or more absorbed power by each bus, it is selected as a common bus because two or more generations are generating power to the corresponding bus. In this example, the rows with two or more negative numbers are #4 and #5 rows, so the #4 and #bus are common bus as shown in Matrix (2) and Fig. 5(a).
2) Perform DFS from generator to common bus. In the corresponding search, the search can proceed only when positive power flow data is found in Matrix (2). For example, #1 generator for #1 row of Matrix (2) can find a positive value '100' at the intersection with #4 column, so that it can be searched by #4 bus. After that, the #4 bus is a common bus, so the search for #1 generator is stopped. The result of searching from all generators is shown in Fig. 5(b).
3) Determine the subdivision group for the next element to which the common bus is connected. The procedure will be explained in detail in Chapter 5.3. Referring to Fig. 5(c), the subdivision group for the

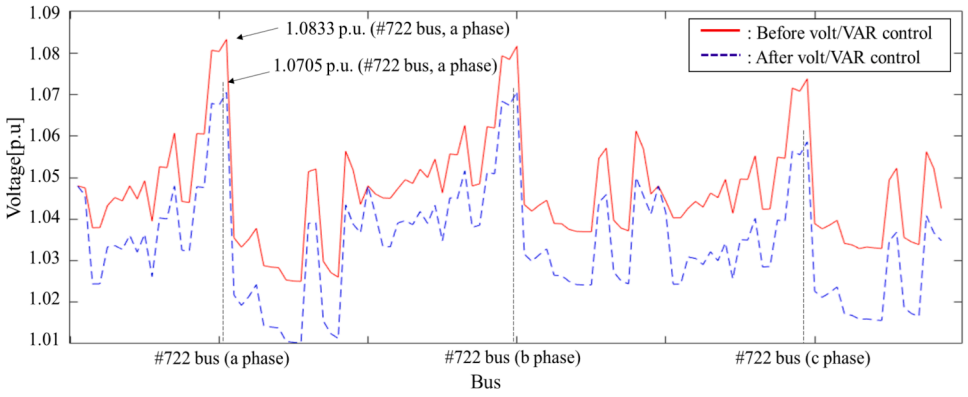

Fig. 14. Comparison of voltage profiles at #722 bus due to volt/VAR control.

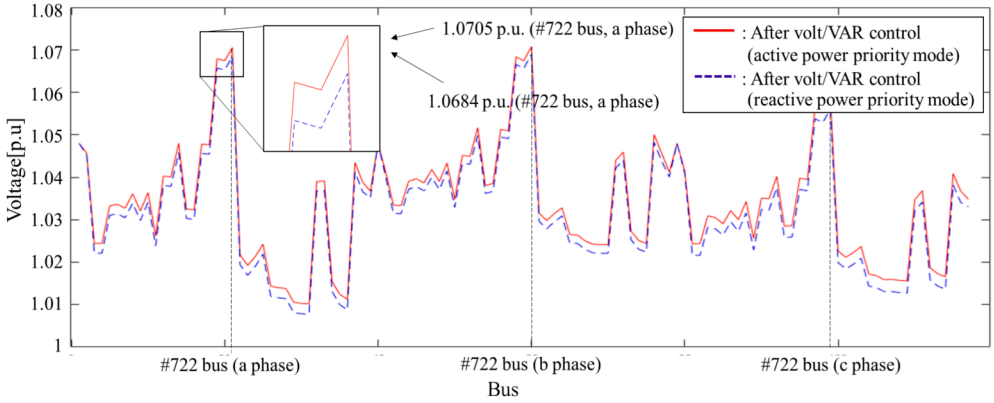

Fig. 15. Comparison of voltage profiles at #722 bus due to priority mode.

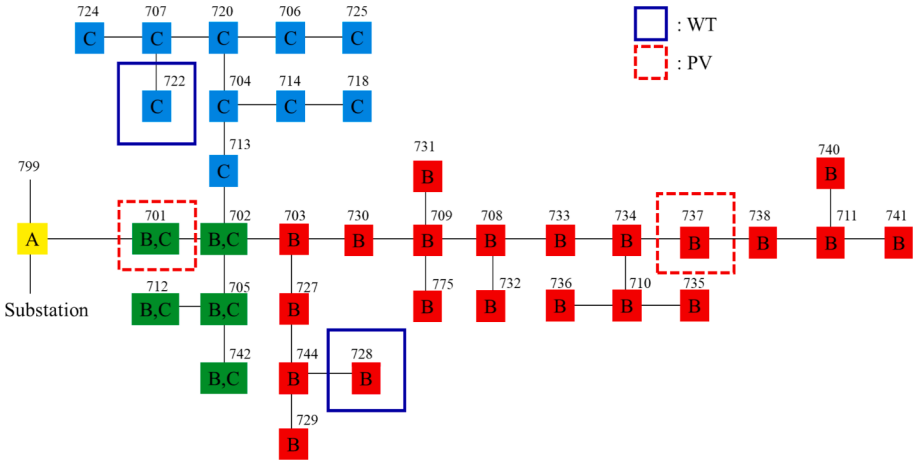

Fig. 16. Subdivision result at time of maximum overvoltage.

connected #4 common bus and #7 load is determined for the #5 common bus.

4) For #4 common bus, the subdivision group for the next connected load #8 is also determined. The corresponding figure is like Fig. 5(d).
5) The subdivision of the next element connected to the common bus is newly determined according to 3), and 4), and DFS is performed again by selecting the corresponding element as the starting point. When there is no more searchable element, the algorithm ends, and if there is still searchable element, the process of 2) ~ 5) is repeated.

In the case of Fig. 5, because it is a simulated system for easy explanation, the subdivision is completed through only steps 2) to 4). However, for large-scale power system, the search process through step 5) should be repeatedly performed again.

4.2. *Determining the subdivision group for the next element to common bus*

The common bus is the intersection of subdivisions because it is the point where the generated power is from each generator. Therefore, if DFS starts again from the common bus having two or more groups, one subdivision is left in the end, and it becomes the same as the existing

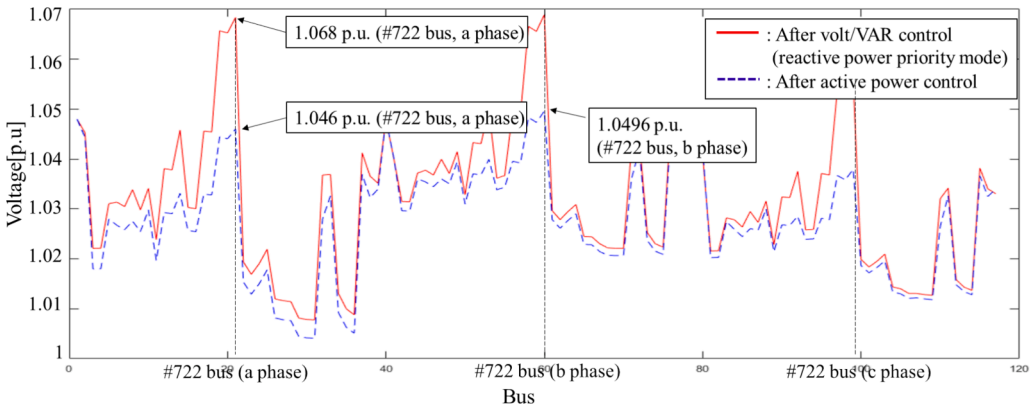

Fig. 17. Voltage profile after performing active power control.

Table 3
Operation status of EVs and DGs for overvoltage of worst case.

Time	PV Volt/VAR		EV Volt/VAR	WT Curtailment		Simulation time
	PV1	PV2		WT1	WT2	
0:00	Q	Q	Q (100 %)	24.8 %	x	0.41 s
0:15	Q	Q	Q (100 %)	12.0 %	x	0.34 s
0:30	Q	Q	Q (100 %)	36.8 %	x	0.49 s
1:30	x	x	P (32 %)	x	x	0.05 s
2:30	Q	Q	Q (100 %)	38.4 %	x	0.52 s
3:15	x	x	P (16 %)	x	x	0.03 s
4:15	Q	P	Q (36 %)	x	x	0.24 s
4:30	x	x	P (8 %)	x	x	0.02 s
4:45	x	x	P (60 %)	x	x	0.12 s
5:30	Q	Q	Q (100 %)	30.5 %	x	0.44 s
6:30	x	x	P (24 %)	x	x	0.05 s
7:45	Q	Q	Q (100 %)	13.9 %	x	0.33 s
8:00	Q	Q	Q (100 %)	41.6 %	x	0.58 s
8:15	Q	Q	Q (100 %)	30.9 %	x	0.44 s
8:45	Q	Q	Q (100 %)	18.3 %	x	0.39 s
10:30	Q	Q	Q (100 %)	13.3 %	x	0.35 s
12:15	Q	Q	Q (100 %)	16.3 %	x	0.37 s
14:00	Q	Q	Q (100 %)	11.2 %	x	0.33 s
14:15	Q	Q	Q (100 %)	20.2 %	x	0.39 s
15:45	Q	Q	Q (100 %)	22.7 %	x	0.41 s
22:00	Q	Q	Q (100 %)	8.1 %	x	0.28 s
23:15	Q	Q	Q (100 %)	28.0 %	x	0.36 s

whole system. Therefore, which group the next element connected to the common bus will be included in is an important issue in the process of subdivision. In this paper, the subdivision group of the next element is determined by matching the absorbed power and injecting power by common bus. Each absorbed power and injecting power in common bus are sorted in descending order, respectively. Also, if the loss isn't considered, each sum of absorbed power and injecting power is the same, so matching is possible as shown in Fig. 6. By proceeding in this way, the subdivision group can be determined on the next element to which power is injected from the common bus.

Therefore, power flow through #5 common bus can express as shown in Fig. 7, and the subdivision belonging to the #4 common bus (subdivision B) and #7 load (subdivision B,C) is determined accordingly. At this time, the process is performed preferentially from the common bus where the group of all absorbed power is determined, and accordingly, in Fig. 5(c), it is performed from the #5 common bus instead of the #4 common bus.

4.3. Proposed Volt/Watt control of EVs and DGs

The proposed active power control is controlled by the volt/Watt characteristic curve and is performed when the voltage problem isn't solved even after performing volt/VAR control preferentially. When an overvoltage occurs, DGs performs volt/Watt control as shown in Fig. 8. And when an undervoltage occurs, EVs perform volt/Watt control as shown in Fig. 9. In addition, since this paper isn't a paper to optimize the volt/Watt characteristic curve, the following general volt/Watt curve is used [20]. Based on characteristic curves, DGs and EVs output power corresponding to the voltage at their associated nodes.

The overall flow chart proposed in this paper is shown in Fig. 10.

5. Simulation conditions and analysis

5.1. Simulation conditions

An IEEE 37-node test system is used for simulation, as shown in

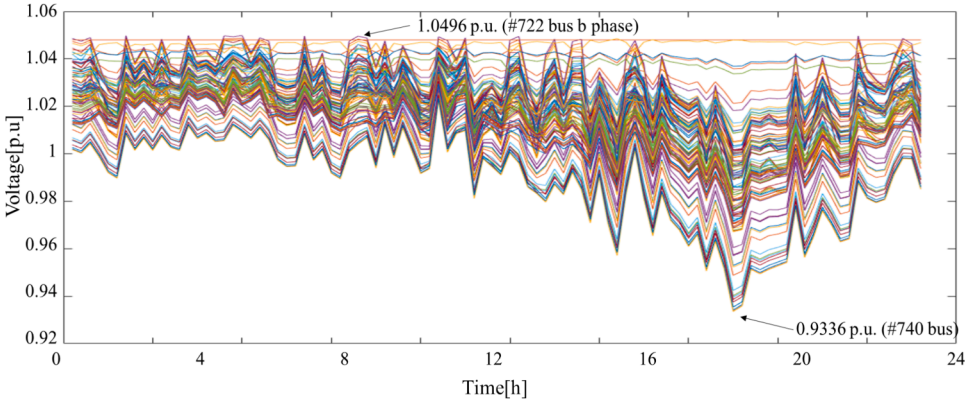

Fig. 18. Voltage profile after applying proposed method to solve overvoltage.

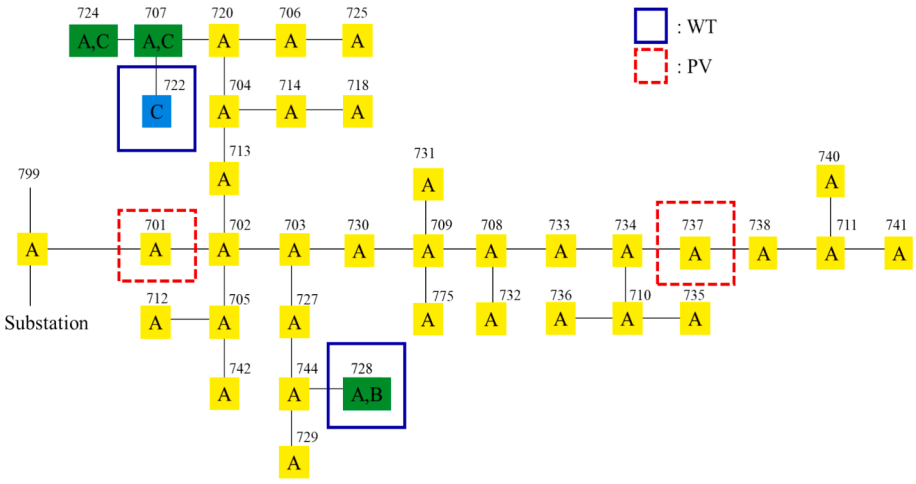

Fig. 19. Subdivision result at time of minimum undervoltage.

Table 4
Bus where undervoltage occurred and corresponding subdivision.

Bus No.	#733	#710	#735	#736	#711
Voltage[p.u.]	0.9488	0.9402	0.9396	0.9386	0.9342
Subdivision	A	A	A	A	A
Bus No.	#741	#740	#734	#737	#738
Voltage[p.u.]	0.9337	0.9336	0.9424	0.9375	0.9354
Subdivision	A	A	A	A	A

Fig. 11. Simulation was performed for one day, and the simulation time step was 15 min. Generally, wind power generators are primarily installed in mountainous or coastal areas. therefore, they were placed at the two nodes with the highest load among the terminal loads. Solar power installations, assuming they are located inland, were positioned at the two nodes with the highest load among the non-terminal nodes. Electric vehicle charging stations were distributed across all nodes with a load, with capacities installed proportionally according to the penetration rate. The daily profile of Wind Turbine (WT), which is installed in #724, #728bus, follows the Weibull distribution, and the daily profile of PV, which is installed in #701, #737bus, follows the beta distribution [21]. The corresponding profile can be seen in Fig. 12. Also, the daily profile of EVs is implemented probabilistically based data surveyed in Jeju Island, Republic of Korea in 2016 as shown in Fig. 12 [21]. To validate the effect of the proposed voltage regulating algorithm on the largest variability, the penetration of the total DGs and EVs are selected as 100 %, respectively. The total load excluding EVs is about 2.735MVA, for the capacity of the EVs for each bus, the total capacity in each simulation case was equally installed in the bus where the existing load was already installed. Each case is simulated by five Intel CPU cores (at 3.50 GHz) and 8 GB RAM.

5.2. Simulation results for coordinated control to solve the overvoltage

As mentioned in the simulation condition, to consider the worst case,

Table 5
Bus searching results from #740 bus.

Order	1	2	3	4	5	6	7	8
No.	#740 bus	#738 bus	#741 bus	PV2	#737 bus	#734 bus	#733 bus	#735 bus
Order	9	10	11	12	13	14	15	16
No.	#732 bus	#730 bus	#731bus	#736 bus	#727 bus	#744 bus	WT2	#728 bus
Order	17	18	19	20	21	22	23	24
No.	#729 bus	#713 bus	#712 bus	#742 bus	#701 bus	PV1	#714 bus	#718 bus
Order	25	26	27	28	29			
No.	#720 bus	#725 bus	WT1	#722 bus	#724 bus			

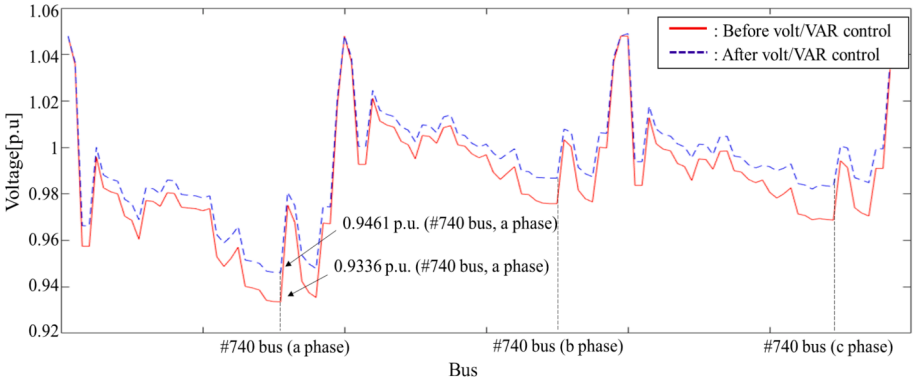

Fig. 20. Comparison of voltage profile at #740 bus due to volt/VAR control.

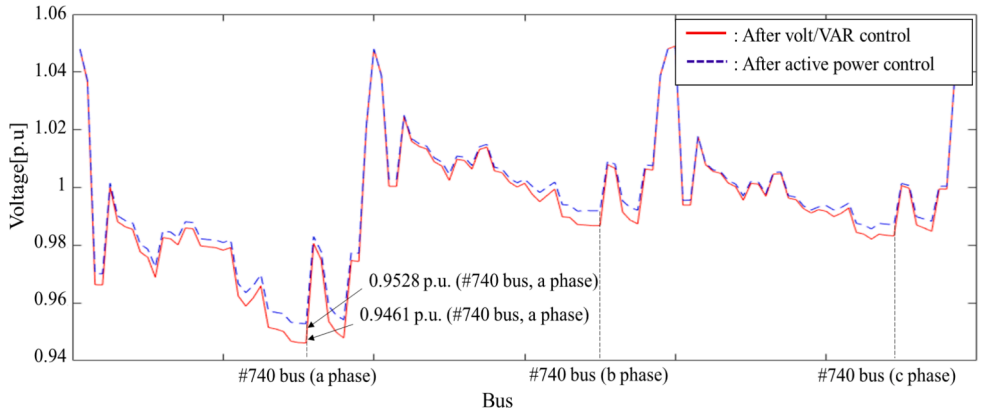

Fig. 21. Voltage profile after performing active power control.

Table 6
Operation status of EVs and DGs for undervoltage of worst case.

Time	PV Volt/VAR		EV Volt/VAR	EV Volt/Watt	Simulation time
	PV1	PV2			
18:30	Q	Q	Q (100 %)	6.9 %	0.04 s
18:45	x	P	P (24 %)	x	0.09 s

the penetration of DGs and EVs are selected as 100 % respectively. The voltage profile for the simulation condition is shown in Fig. 13, and largest overvoltage and lowest undervoltage occur in the #722 and #740 bus.

At this time, the procedure for controlling the proposed algorithm for the time when the largest overvoltage has occurred is as follows. Since the largest overvoltage occurs in #722 bus, it can be determined that WT1 causes overvoltage according to connection information of Fig. 10. Therefore, if the BFS is performed from WT1, the search results shown in Table 2 are obtained.

If the volt/VAR control is performed through active power priority mode in the order of Table 2, it can be seen that the maximum overvoltage of 1.0833p.u. is reduced to 1.0705p.u. as shown in Fig. 14. In the case of active power priority mode, because the magnitude of overvoltage is too high, the overvoltage could not be completely resolved even if all DGs and EVs perform volt/VAR control.

Since the overvoltage is not completely solved in the active power priority mode, volt/VAR control is performed again through the reactive power priority mode. However, in this, case, the amount of EV and PV is not large at the time of the overvoltage, so even if the reactive power priority mode is performed, the effect of voltage regulating is insufficient as shown in Fig. 15, because the change in the output of reactive power is small.

If the voltage problem is not solved even after the reactive power control is completed, the active power is controlled thereafter. Fig. 16 shows the subdivision result at the time of the maximum overvoltage. According to Fig. 11, PV does not work at time of maximum overvoltage because it was early morning. And since the amount of generated power by WT is very high as shown in Fig. 11, WT generates the required whole power by power system. Therefore, the WT, in the subdivision C including the #722 bus where the overvoltage occurs, controls the active power. Finally, after controlling the active power, the voltage is maintained within the normal range as shown in Fig. 17.

As such, the proposed algorithm in this paper is performed when overvoltage occurs, and Table 3 shows how much the EVs and DGs participates in voltage control at the time when overvoltage occurs.

In Table 3, EVs and DGs which do not operate are indicated by 'x'. Also, in the case of volt/VAR control, it is specified as 'P' when operating at active priority mode, and specified as 'Q' when operating at reactive priority mode. Finally, in the case of EV's volt/VAR control, the participation of the EVs in voltage control is expressed as a percentage, and in the case of the WT, the ratio of the curtailed active power is expressed as a percentage.

If the control as shown in Table 3 is performed through the proposed algorithm, it can be confirmed that all overvoltages are solved as shown in Fig. 18. In the simulation, control is performed within 0.32 s on

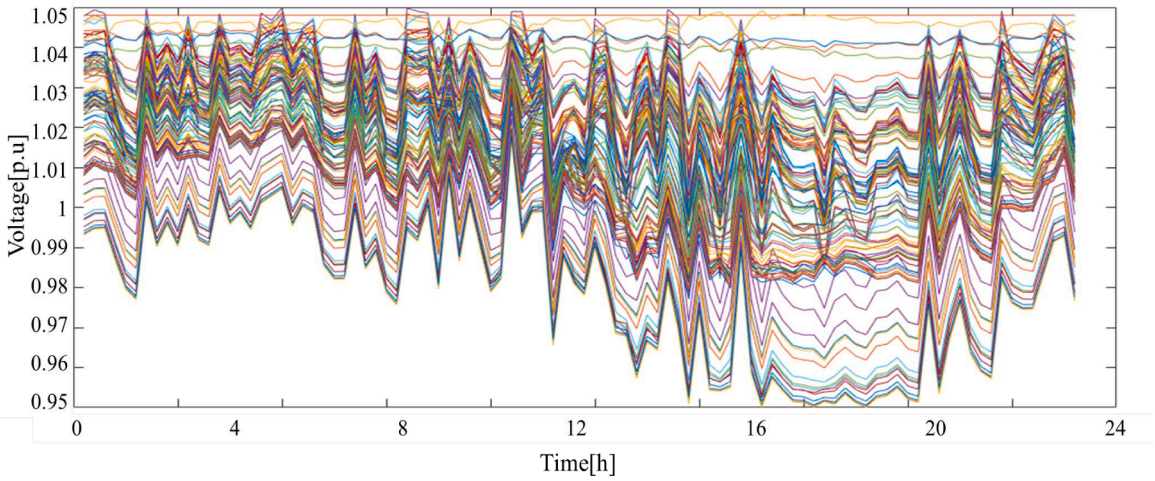

Fig. 22. Voltage profile after performing whole proposed algorithm.

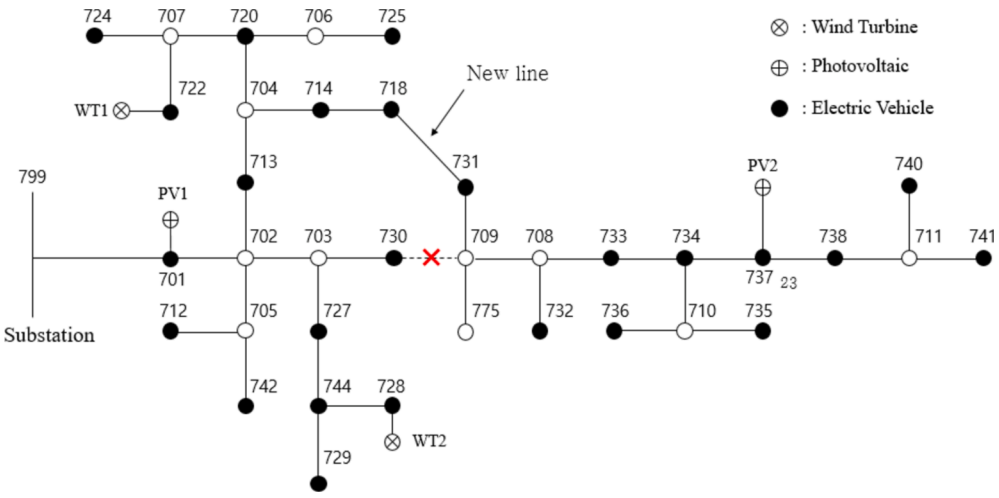

Fig. 23. Example of changed system topology for BFS.

Table 7
BFS results from WT1 according to modified system topology.

Order	1	2	3	4	5	6	7	8
No.	WT1	#722bus	#724bus	#720bus	#725bus	#714bus	#713bus	#718bus
Order	9	10	11	12	13	14	15	16
No.	#731bus	#712bus	#742bus	#701bus	PV1	#732bus	#733bus	#727bus
Order	17	18	19	20	21	22	23	24
No.	#734bus	#744bus	#730bus	#728bus	WT2	#729bus	#737bus	PV2
Order	25	26	27	28	29			
No.	#735 bus	#738 bus	#740 bus	#736 bus	#741 bus			

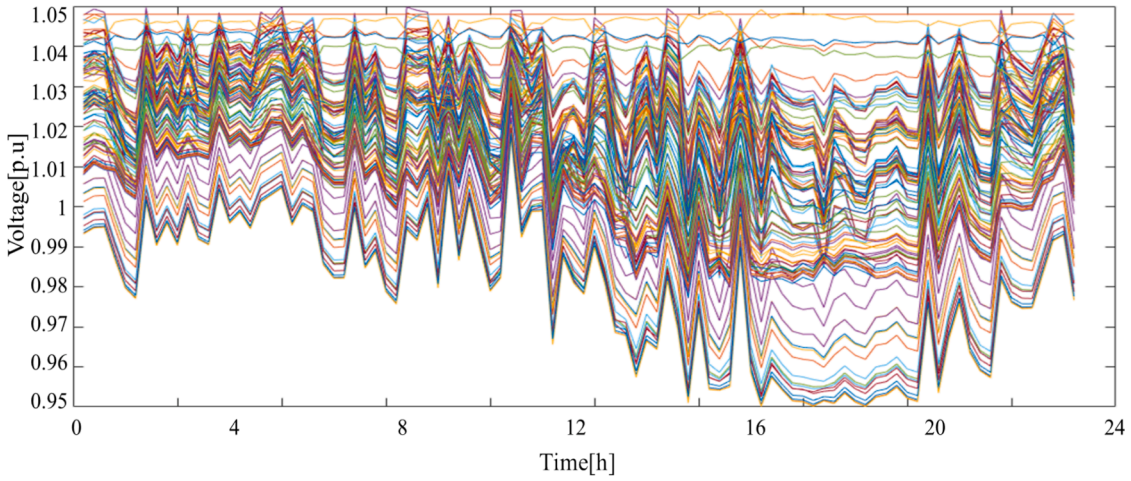

Fig. 24. Voltage profile for changed topology after applying proposed method.

average for each time period even in the worst case. In particular, when the magnitude of the overvoltage is not seriously large, the voltage is regulated only by reactive power. In this case, the simulation time is less than 0.05 s.

5.3. Simulation results for coordinated control to solve the undervoltage

As shown in Fig. 13, the lowest undervoltage occurs at 18:30. As can be seen from Fig. 11, since the generation of DG at that time is very low, the main source is responsible for most of the area as shown in Fig. 19.

At this time, the bus where the undervoltage occurs and the corresponding subdivision are shown in Table 4. Proposed algorithm selects the bus with the lowest voltage for each subdivision as the starting point of BFS. Therefore, #740 bus becomes the starting point of the BFS. The corresponding search order is shown in Table 5.

If the reactive power is controlled in the order of Table 5, the conventional undervoltage (0.9336p.u.) at #740 bus, rises to 0.9461p.u. as shown in Fig. 20.

Since the undervoltage situation has not yet been completely solved, it should be solved by reducing the charging amount of EVs. Therefore, according to the proposed algorithm, the EVs, in the subdivision A where the undervoltage occurs, perform volt/Watt control together. As a result, the undervoltage is solved as shown in Fig. 21.

As such, the proposed algorithm is performed when undervoltage occurs, and Table 6 shows how much the EVs and DGs participated in voltage control in undervoltage situation. EV Volt/Watt specifies the

Table 8
Comparing results of each algorithm for daily profile.

Algorithm	Voltage standard deviation[p.u]	System Loss [kVA]	Total simulation time
Genetic algorithm [13,14]	0.0172	402	4 h 34 *m*
Particle swarm optimization [9,18]	0.0170	387	3 h 22 *m*
Robust optimization [15]	0.0164	370	2 h 58 *m*
Bi-level optimization [10]	0.0160	370	2 h 50 *m*
Proposed Algorithm	0.0170	366	13 s

rate at which the EV's charge is reduced. If the control as shown in Table 6 is performed through the proposed algorithm, it can be confirmed that all voltage problems are solved as Fig. 22.

In this way, it can be observed that both overvoltage and undervoltage issues are effectively controlled and resolved according to the flowchart presented in Fig. 10.

5.4. Simulation results for changing of system topology

In order to verify the performance of the proposed algorithm for the topology change of the distribution system, the existing IEEE 37 bus test system as shown in Fig. 10 is changed as shown in Fig. 23. #718 and #731 bus are connected, and the existing line between #730 and #709 bus is disconnected. When the corresponding information is obtained from the central system, the power flow and distance information at the intersection of the rows and columns corresponding to the #730 and #709 bus in the conventional system matrix is set to 0. And for the newly connected #718 and #731 bus, the power flow and distance information is applied to the intersection of the corresponding row and column in the system matrix.

In this way, if only system matrix is changed, EVs and DGs can be searched through the same search algorithm when a voltage problem occurs. Table 7 shows the search results using the BFS is Section 3 when WT1 causes overvoltage. In this way, the algorithm is performed robustly to the system topology change because it is possible to immediately find the adjacent DGs and EVs. Therefore, even if the system changes, as the proposed algorithm adapts in real time, voltage control is performed smoothly as shown in Fig. 24.

5.5. Simulation results compared optimization algorithm for volt/VAR characteristic curve

Since subject of this paper is real-time voltage control using EVs and DGs, the results are compared with the conventional real-time voltage control using optimization algorithm. All of conventional research uses a method that optimizes volt/VAR characteristic curves for smart stations and smart inverters of EVs and PVs. However, only the reactive powers of DGs and EVs are controlled, so the voltage problem is not solved for the simulation conditions of this paper in which the DGs with high penetration are connected. Therefore, active power control is used in the same way through the proposed method in this paper, and the results of optimization algorithm for the purpose of minimizing voltage standard deviation and system loss are compared with the results of the proposed algorithm in Table 8. At this time, a genetic algorithm is used as the optimization algorithm, and the number of generations of the genetic algorithm is set to 30, and the optimal volt/VAR characteristic curve for each EV is selected by performing 1,000 iterations.

The proposed algorithm shows no significant difference in voltage standard deviation and shows the best performance in reducing losses. This is an advantage because when the optimization algorithm is used, all EVs continuously performs voltage control through continuous voltage monitoring at bus, but in the proposed algorithm, control is activated for specified EVs only when a voltage problem occurs. In addition, regarding simulation speed, it showed superior performance compared to the optimization algorithm. As shown in Table 8, the simulation time of the optimization algorithm is very long. Therefore, it takes a very long time to select a new optimized volt/VAR characteristic curve for the system topology change. To confirm the result of the changed system topology, it is assumed that the line between #703 and #730 is disconnected and #728 and #732 bus are newly connected as shown in Fig. 25. This scenario considers a fault between #703 and #730. In response, the distribution automation system assumes that the

Table 9
Comparing results according to modified system topology.

Algorithm	Voltage standard deviation[p.u]	System Loss [kVAh/day]
Genetic algorithm [13,14]	0.0212	443
Particle swarm optimization [9,18]	0.0210	432
Robust optimization [15]	0.0208	433
Bi-level optimization [10]	0.0213	420
Proposed Algorithm	0.0193	349
Comparison of results with optimization with the best performance	−7.21 %	−16.90 %

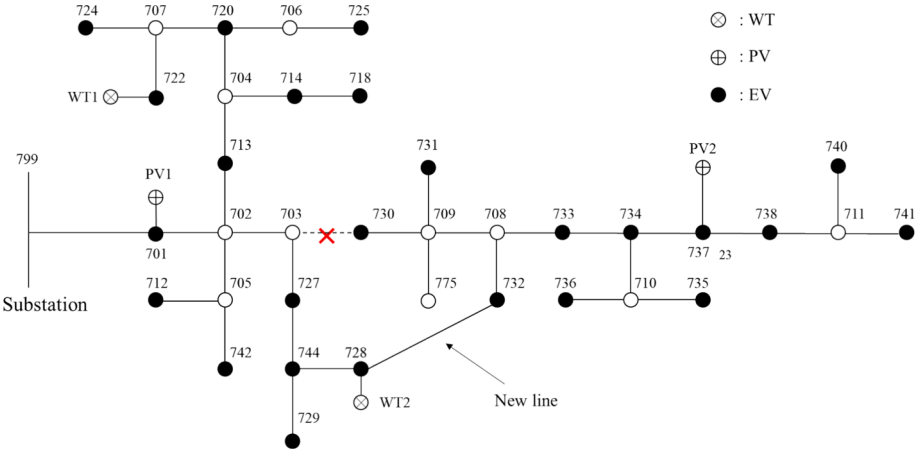

Fig. 25. Example of changed system topology for comparing results.

line is blocked and closes the circuit breaker between #728 and #732 to maintain power supply to the main source and the lower level system.

At this time, the Table 9 compares the results of using the existing volt/VAR characteristic curve which obtained by the optimization algorithm before the system topology change, and the results of the proposed algorithm in which is implemented by adapting to the system topology change. From results, it can be confirmed that the optimal volt/VAR characteristic curve through the optimization algorithm cannot be accurately controlled when the system topology is changed. However, the proposed algorithm performed smoothly, and thus showed improved results in terms of voltage deviation and system loss reduction than the optimization algorithm. In particular, after the system topology was changed, the proposed algorithm did not optimally reduce the voltage deviation because re-optimization did not occur as it would in an optimization algorithm. However, since the proposed algorithm is applied in real time, it reduced the voltage deviation by 7.21 % compared to the optimization algorithm. Moreover, the system losses decreased significantly by 16.90 %, demonstrating the advantages of the proposed approach. As a result, proposed algorithm has the flexibility to the system topology change.

6. Conclusions

In this paper, new coordinated voltage regulating method between EVs and DGs is developed. By using GSM, the priority for reactive power control is selected for the DGs and EVs. The voltage control is sequentially performed according to the priority. As a result, it is confirmed that the voltage problem could be solved only with specific EVs and DGs, and losses could also be reduced. Also, even if the topology of distribution system is changed, the proposed algorithm is performed without any additional consideration. Because the topology of the distribution system can change according to the system situation due to the distribution automation system, an adaptive algorithm which can be applied is required.

Through the proposed algorithm, adaptive voltage regulating is possible even in the distribution system connected with large-scale DGs and EVs, and stable voltage can be supplied to consumers. And in this paper, only coordination control between EVs and DGs is performed, but other voltage regulators such as capacitor banks or energy storage systems in the distribution system. Since the proposed algorithm in this paper is a method to find the adjacent voltage regulator to the area where the voltage problem occurs using the GSM, coordinated control with other voltage regulators can also be expected. In addition, as distribution systems become increasingly complex, resolving voltage issues using existing optimization algorithms inevitably requires more time. However, the algorithm proposed in this paper offers a significant advantage in terms of speed. It addresses voltage problems locally and rapidly at the point where the issue arises, thereby enhancing problem-solving efficiency. Finally, it supports the connection of large-capacity DGs and EVs to the distribution system by controlling the voltage, which is the biggest factor determining the hosting capacity, which means the total capacity of the DGs which can be maximally connected to the distribution system.

CRediT authorship contribution statement

Jisoo Kim: Writing – original draft, Data curation, Conceptualization. **Jean Mahseredjian:** Writing – review & editing.

Declaration of competing interest

The authors declare that they have no known competing financial interests or personal relationships that could have appeared to influence the work reported in this paper.

Data availability

No data was used for the research described in the article.

Acknowledgements

This work has been supported by the National Research Foundation of Korea (NRF) grant funded by the Korean government (MSIP) (No. 2021R1A2B5B03086257)

References

[1] Lee SJ, Kim JH, Kim CH, Kim SK, Kim ES, Kim DU, Mehmood KK, Khan SU. Coordinated control algorithm for distributed battery energy storage systems for mitigating voltage and frequency deviations. IEEE Trans Smart Grid 2015;7(3):1713–22.
[2] Cho G-J, Kim C-H, Yun-Sik Oh, Kim M-S, Kim J-S. Planning for the future: optimization-based distribution planning strategies for integrating distributed energy resources. IEEE Power Energ Mag 2018;16(6):77–87.
[3] Gush T, Kim C-H, Admasie S, Kim J-S, Song J-S. Optimal smart inverter control for PV and BESS to improve PB hosting capacity of distribution networks using slime mould algorithm. IEEE Access 2021;9:52164–76.
[4] Daratha N, Das B, Sharma J. Coordination between OLTC and SVC for voltage regulation in unbalanced distribution system distributed generation. IEEE Trans Power Syst 2013;29(1):289–99.
[5] Te-Tien Ku, Lin C-H, Chen C-S, Hsu C-T. Coordination of transformer on-load tap changer and PV smart inverters for voltage control of distribution feeders. IEEE Trans Ind Appl 2019;55(1):256–64.
[6] Liu X, Aichhorn A, Liu L, Li H. Coordinated control of distributed energy storage system with tap changer transformers for voltage rise mitigation under high photovoltaic penetration. IEEE Trans Smart Grid 2012;3(2):897–906.
[7] Singh P, Bishnoi SK, Meena NK. Moth Search Optimization for optimal DERs integration in conjunction to OLTC Tap operations in distribution systems. IEEE Syst J 2020;14(1):880–8.
[8] IEEE, "1547-2018 - IEEE standard for interconnection and interoperability of distributed energy resources with associated electric power systems interfaces", 2018.
[9] Jin D, Chiang H-D, Li P. Two-timescale multi-objective coordinated volt/var optimization for active distribution networks. IEEE Trans Power Syst 2019;34(6):4418–28.
[10] Jha RR, Dubey A, Liu CC, Schneider KP. Bi-level volt-var optimization to coordinate smart inverters with voltage control devices. IEEE Trans Power Syst 2019;34(3):1801–13.
[11] Majumdar A, Agalgaonkar YP, Pal BC, Gottschalg R. Centralized volt–var optimization strategy considering malicious attack on distributed energy resources control. IEEE Trans Sustain Energy 2017;9(1):148–56.
[12] Kim KH. Decentralized power management of DC microgrid based on adaptive droop control with constant voltage regulation. IEEE Access 2022;10:129490–504.
[13] Das D, Manojkumar R, Kumar C, Ganguly S. Power loss minimization in smart transformer enabled low voltage islanded meshed hybrid microgrid. IEEE Access 2022;10:123259–70.
[14] Wang J, Bharati GR, Paudyal S, Ceylan O, Bhattarai BP, Myers KS. Coordinated electric vehicle charging with reactive power support to distribution grids. IEEE Trans Ind Inf 2019;15(1).
[15] Pirouzi S, Aghaei J, Latify MA, Reza Yousefi G, Mokryani G. A robust optimization approach for active and reactive power management in smart distribution networks using electric vehicles. IEEE Syst J 2018;12(3):2699–710.
[16] Mazumder M, Debbarma S. EV charging stations with a provision of V2G and voltage support in a distribution network. IEEE Syst J 2021;15(1):662–71.
[17] Prabawa P, Choi D-H. Hierarchical volt-var optimization framework considering voltage control of smart electric vehicle charging stations under uncertainty. IEEE Access 2021;9:123398–413.
[18] Singh S, Pamshetti VB, Singh SP. Time horizon-based model predictive Volt/VAR optimization for smart grid enabled CVR in the presence of electric vehicle charging loads. IEEE Trans Ind App 2019;55(6):5502–13.
[19] Quijano DA, Padilha-Feltrin A, Catalão JPS. Volt-var optimization with power management of plug-in electric vehicles for conservation voltage reduction in distribution systems. IEEE Trans Ind App 2023;60(1):1454–62.
[20] J. Duncan Glover, Mulukutla S. Sarma and Thomas J. Overbye, "Power system analysis and design, fifth edition", (2012) 268-272.
[21] Kim J-S, Kim C-H, Yun-Sik Oh, Cho G-J, Song J-S. An islanding detection method for multi-RES systems using the graph search method. IEEE Trans Sustain Energy 2020;11(4).